SCIENCE CHINA
Earth Sciences

•ARTICLE•

February 2024 Vol.67 No.2: 387–404
https://doi.org/10.1007/s11430-023-1217-8

Counteracting effects on ENSO induced by ocean chlorophyll interannual variability and tropical instability wave-scale perturbations in the tropical Pacific

Rong-Hua ZHANG[1,2,4*], Feng TIAN[2,3], Qidong SHI[3,4], Xiujun WANG[5] & Tongwen WU[6]

[1] *School of Marine Sciences, Nanjing University of Information Science and Technology, Nanjing 210044, China;*
[2] *Laoshan Laboratory, Qingdao 266237, China;*
[3] *Key Laboratory of Ocean Circulation and Waves, Institute of Oceanology, Chinese Academy of Sciences, Qingdao 266071, China;*
[4] *University of Chinese Academy of Sciences, Beijing 101408, China;*
[5] *Faculty of Geographical Sciences, Beijing Normal University, Beijing 100875, China;*
[6] *Earth System Modeling and Prediction Centre, China Meteorological Administration, Beijing 100081, China*

Received January 29, 2023; revised August 29, 2023; accepted October 30, 2023; published online December 6, 2023

Abstract Large perturbations in chlorophyll (Chl) are observed to coexist at interannual and tropical instability wave (TIW) scales in the tropical Pacific; at present, their combined effects on El Niño-Southern Oscillation (ENSO) through ocean biology-induced heating (OBH) feedbacks are not understood well. Here, a hybrid coupled model (HCM) for the atmosphere and ocean physics-biogeochemistry (AOPB) in the tropical Pacific is adopted to quantify how ENSO can be modulated by Chl perturbations at interannual and TIW scales, individually or collectively, respectively. The HCM-based sensitivity experiments demonstrate a counteracting effect on ENSO: the bio-climate feedback due to large-scale Chl interannual variability acts to damp ENSO through its impact on upper-ocean stratification and vertical mixing, whereas that due to TIW-scale Chl perturbations tends to amplify ENSO. Because ENSO simulations are sensitively dependent on the ways Chl effects are represented at these different scales, it is necessary to adequately take into account these related differential Chl effects in climate modeling. A bias source for ENSO simulations is illustrated that is related with the Chl effects in the tropical Pacific, adding in a new insight into interactions between the climate system and ocean ecosystem on different scales in the region. These results reveal a level of complexity of ENSO modulations resulting from Chl effects at interannual and TIW scales, which are associated with ocean biogeochemical processes and their interactions with physical processes in the tropical Pacific.

Keywords Ocean chlorophyll, Bio-climate feedbacks, Interannual variability, Tropical instability waves, Counteracting effects, A hybrid coupled model

Citation: Zhang R H, Tian F, Shi Q, Wang X, Wu T. 2024. Counteracting effects on ENSO induced by ocean chlorophyll interannual variability and tropical instability wave-scale perturbations in the tropical Pacific. Science China Earth Sciences, 67(2): 387–404, https://doi.org/10.1007/s11430-023-1217-8

1. Introduction

The El Niño-Southern Oscillation (ENSO) phenomenon exhibits a varying amplitude. Despite previous intensive and extensive studies, the mechanisms for ENSO diversity and complexity are still not understood well (e.g., Zhang et al., 1998; Collins et al., 2010; Zhu et al., 2012; Chen et al., 2015). Previously, a focus has been intensively placed on physical aspects (Zhu et al., 2014; Hu et al., 2017; Kang et al., 2017; Lian et al., 2017). In the past two decades, ocean biogeochemistry in the tropical Pacific has also been demonstrated to play a role in ENSO modulations (e.g., Murtugudde et al., 2002; Timmermann and Jin, 2002; Miller et al., 2003; Wetzel et al., 2006; Gnanadesikan and Anderson,

* Corresponding author (email: rzhang@nuist.edu.cn)

2009; Zhang et al., 2009; Jochum et al., 2010; Park et al., 2014; Kang et al., 2017; Shi et al., 2023). Indeed, as a biological signature clearly evident from available satellite observations, ocean chlorophyll (Chl) field exhibits large perturbations at different space-time scales in the tropical Pacific.

At interannual time scales associated with ENSO cycles, Chl undergoes large-scale variations in the equatorial Pacific, which not only represents a response to ENSO, but also induces a feedback onto ENSO (e.g., Zhang et al., 2009, 2019a). A negative feedback onto ENSO has been illustrated due to interannually varying Chl effects in the tropical Pacific (Zhang, 2015). Furthermore, it has been illustrated that the ocean biology-induced feedback is realized mainly by its indirect effects on the upper ocean dynamics through redistribution of penetrative solar radiation; the induced vertical differential heating and density field in the mixed layer (ML) and subsurface layers act to modulate the stratification and vertical mixing in the upper ocean, which influences SST and thus ENSO.

At intraseasonal scales, tropical instability waves (TIWs) are small-scale phenomena that are pronouncedly seen in the eastern tropical Pacific (e.g., Legeckis, 1977). As has been long recognized for being an important component in the tropical Pacific climate system, TIWs influence the oceanic heat and momentum transports near the equator (e.g., Bryden and Brady, 1989; Baturin and Niiler, 1997; Kessler et al., 1998; Zhang, 2014). Satellite data indicate that TIWs are accompanied with large perturbations not only in physical fields, but also in ocean biogeochemistry (Chavez et al., 1999; Strutton et al., 2001; Legeckis et al., 2004; Gorgues et al., 2005). A positive feedback onto ENSO has been recently demonstrated through TIW-induced Chl perturbations (Tian et al., 2018, 2019), acting to perturb density field in the upper ocean, which affects the exchange between eddy potential energy (EPE) and eddy kinetic energy (EKE). These processes in turn tend to modulate TIWs themselves, which further affect the meridional heat transport onto the equator in the eastern tropical Pacific, leading to an SST change in the cold tongue and thus impacts on ENSO.

ENSO and TIWs are two prominent phenomena involving air-sea coupling in the tropical Pacific. Accompanied with them, large Chl perturbations are observed to coexist at these different scales in the region; correspondingly, their effects on the mean climate and interannual variability are expected in the tropical Pacific. For example, interannual Chl effects have been examined using coupled ocean-atmosphere models, including highly idealized concept models (e.g., Timmermann and Jin, 2002), HCMs (Marzeion et al., 2005; Zhang et al., 2009), and coupled general circulation models (e.g., Wetzel et al., 2006; Lengaigne et al., 2007; Gnanadesikan and Anderson, 2009; Jochum et al., 2010; Park et al., 2014). Results indicate that the induced bio-effects on the climate simulations are strongly model dependent, with significant intermodel differences. At TIW scales, physical aspects of TIW-induced effects on the climate in the tropical Pacific have been understood quite well (e.g., Menkes, 2002; Zhang, 2014; Holmes et al., 2019); but their biological aspects and corresponding roles in ENSO modulations through the ocean ecosystem are still poorly understood (Tian et al., 2018). In particular, TIW-induced bio-effects on ENSO and their interactions with interannually varying Chl feedback remain elusive. At present, large uncertainties exist in representing and understanding Chl effects at interannual and TIW scales in the tropical Pacific. Due to the roles played by TIWs in the climate system and ocean ecosystem in the tropical Pacific, it is important to understand TIW-scale Chl effects and their interactions with physical processes at interannual scales.

Previously, we have illustrated the Chl-related feedback effects on ENSO using a coupled model of the atmosphere and ocean physics-biogeochemistry (AOPB), in which pronounced TIW and interannual Chl signals are captured in simulations (Tian et al., 2018, 2019; Zhang et al., 2018, 2019a). Clear interactions are seen between physical and biogeochemistry processes at different scales. Because Chl perturbations at interannual and TIW scales are collectively represented in the coupled modeling system, it is difficult to unambiguously separate the TIW-induced Chl roles in ENSO modulations in the presence of interannually varying Chl feedback effects.

In this study, the HCM AOPB is used to perform sensitivity experiments to quantify individual and collective effects on ENSO due to TIW-induced Chl perturbations (Chl_{TIW}) and Chl interannual variability (Chl_{inter}), respectively. Since the ocean ecosystem model can explicitly simulate Chl fields (including TIW and interannually varying signals), their corresponding TIW and interannual Chl effects on upper-ocean temperature calculations associated with the penetrative solar radiation can be alternatively considered or not, allowing their effects on ENSO to be quantified in a clear way.

2. Model descriptions and experimental designs

In this work, a hybrid coupled model (HCM AOPB) is formed to represent the bio-climate interactions in the tropical Pacific (Figure 1): an ocean ecosystem model is further incorporated into an atmosphere-ocean coupled model (representing the climate system). For example, the total wind stress (τ) is separated into its climatological part (τ_{clim}), interannual anomalies (τ_{inter}) and TIW-induced wind stress perturbations (τ_{TIW}), written as $\tau=\tau_{clim}+\alpha_{\tau}\cdot\tau_{inter}+\tau_{TIW}$. A statistical model for τ_{inter} is constructed using a singular value decomposition (SVD) analysis technique between inter-

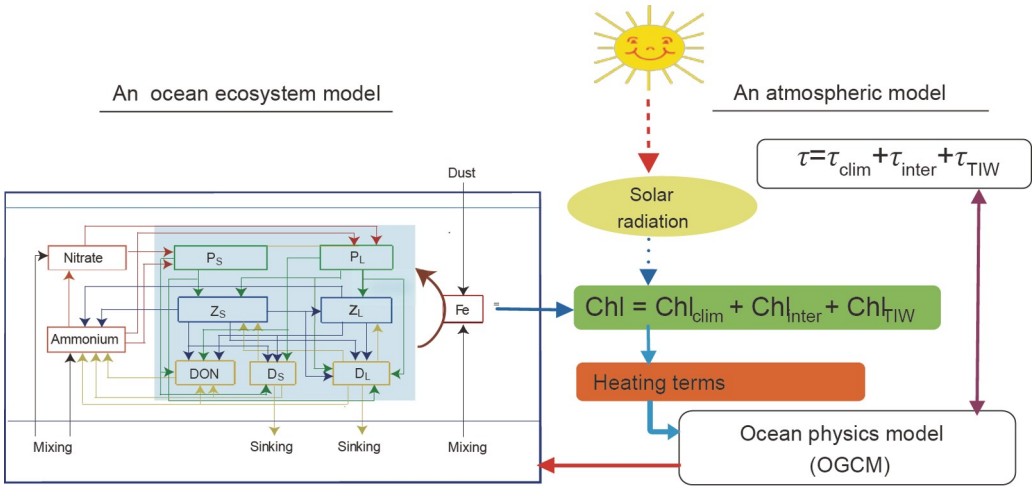

Figure 1 A schematic diagram illustrating a hybrid coupled model (HCM) used to represent the interactions among the atmosphere, ocean physics and biogeochemistry (AOPB) in the tropical Pacific. The HCM AOPB consists of statistical atmospheric models for wind stress, an OGCM and an ocean biogeochemistry model.

annual anomalies of SST and τ, in which α_τ is a scalar coefficient introduced to represent the strength of the corresponding wind forcing; a statistical model for τ_{TIW} is also constructed using SVD analysis technique between TIW-induced perturbations of SST and τ derived from satellite observations. Furthermore, the climate system is coupled with an ocean biology model that determines chlorophyll (Chl), which affects the penetration of solar radiation in the upper ocean. Correspondingly, the total Chl can be also separated into its climatological part (Chl_{clim}), interannual anomalies (Chl_{inter}) and TIW-induced perturbations (Chl_{TIW}), written as $Chl=Chl_{clim}+Chl_{inter}+Chl_{TIW}$. In this simplified coupled system, some climatological fields are prescribed to be seasonally varying (e. g., τ_{clim} and SST_{clim}) and interannual anomalies are determined by departures from their corresponding climatological fields (e. g., $SST_{inter}=SST-SST_{clim}$, in which SST_{clim} is climatological SST). Interactions between the ocean and atmosphere are realized by relationships between SST and wind stress/heat flux/freshwater flux; those between the ocean physics and biology are represented by the related heating terms that are modulated by Chl. Also, TIW-induced wind and Chl feedbacks onto the ocean are represented so that TIW-scale interactions between SST_{TIW} and τ_{TIW} and between Chl_{TIW} and SST_{TIW} are taken into account. The model is briefly described in this section; a more detailed description for the various model components is presented in Zhang et al. (2018, 2020).

2.1 The model used

The oceanic model is an oceanic general circulation model (OGCM), which is the primitive equation, sigma-coordinate model originally developed by Gent and Cane (1989); this model has been extensively used for tropical ocean-atmosphere modeling (e.g., Murtugudde et al., 2002; Wang et al., 2009; Zhang et al., 2012; Gao et al., 2020). The atmospheric fields used to force the OGCM consists of surface wind stress (τ), freshwater flux (FWF) and heat flux; here, FWF at the atmosphere-ocean interface is defined as the difference between precipitation (P) and evaporation (E), with net FWF into the ocean being defined to be positive. The coupling of the OGCM with the simplified atmospheric model forms a hybrid coupled model for the climate system of the tropical Pacific (e.g., Zhang et al., 2012). In such an HCM, the total wind stress field can be separated into three parts, which are written as $\tau=\tau_{clim}+\alpha_\tau\cdot\tau_{inter}+\tau_{TIW}$. Here, τ_{clim} is a prescribed seasonally-varying climatological wind stress field, τ_{inter} is large-scale interannual wind stress anomalies, and τ_{TIW} is TIW-scale wind stress perturbations (Zhang and Busalacchi, 2009a). In a similar way, the total FWF can be written as $FWF=FWF_{clim}+FWF_{inter}$ in which FWF_{clim} is a climatological part and FWF_{inter} is an interannual anomaly part; the FWF effect at TIW scales is not considered here because its signal is not coherent and systematic, with its effect being supposed to be not strong. The corresponding climatological parts (τ_{clim} and FWF_{clim}) are prescribed using their long-term seasonally varying fields from observations; the corresponding τ_{inter} and FWF_{inter} parts (interannual anomalies) are associated with interannual SST anomalies (SST_{inter}), whose relationships are determined using their statistical models constructed by singular value decomposition (SVD) analysis techniques from historical data (Zhang and Gao, 2016; Zhang and Busalacchi, 2009b). The total heat flux forcing the OGCM at the atmosphere-ocean interface is determined by an advective atmospheric mixed layer (AML) model which interactively calculates the heat flux from SST and other atmospheric fields; its details are described in Murtugudde et al. (2002).

In this study, TIWs-induced effects are taken into account in the HCM AOPB. Here, TIW signals are represented in

terms of space-scale perturbations rather than time-scale variations; that is, TIW-scale signals actually stand for a spatial perturbation as has been characterized by previous studies (Chelton et al., 2001; Hashizume et al., 2001; Xie, 2004). To this end, TIW-induced signals in the ocean (e.g., SST_{TIW} for SST and Chl_{TIW} for Chl) can be extracted spatially from their original total fields using a zonal high-passed filter in two steps (Hashizume et al., 2001). First, a large-scale background field is formed by performing a 12° zonal moving average (12° longitudes) of the original field; then, a TIW-scale perturbation field is obtained by subtracting the large-scale background field from its original field. On the atmospheric side, TIW-induced surface wind stress perturbations (τ_{TIW}) are also referred to spatially small scale, instead of temporally high frequency; a surface wind stress model for TIW scale (τ_{TIW}) is constructed using a SVD analysis from satellite data for the eastern tropical Pacific (Zhang, 2014). In this way, TIW-scale surface wind-SST feedback can be represented in the HCM AOPB over the eastern tropical Pacific, involving interactions between the ocean and atmosphere on TIW scales. For example, TIW-induced SST perturbations (SST_{TIW}) in the OGCM can be obtained using the zonal high-pass filter that is applied to daily total SST fields. Then, given an SST_{TIW} field simulated from the OGCM, the τ_{TIW} fields are obtained using the constructed empirical τ_{TIW} model, which are then combined with τ_{clim} and τ_{inter} to form the total τ field to force the ocean, with the τ_{TIW} effect thus being explicitly included in the context of the HCM modeling.

Moreover, an ocean ecosystem model (representing biogeochemistry processes) is incorporated into the climate system (the HCM) to represent bio-climate interactions (HCM AOPB; Zhang et al., 2018). As shown in Figure 1, an ocean ecosystem model is mainly composed of two parts (Wang et al., 2015, 2009): one for biological part, and the other for nutrient part. The former consists of six biological components (large and small sizes of phytoplankton (P_L and P_S), large and small sizes of zooplankton (Z_L and Z_S), and large and small sizes of detritus (D_L and D_S)); the letter consists of six nutrients (nitrate, silicon, ammonium, dissolved inorganic carbon (DIC), dissolved oxygen, and dissolved iron, respectively). In addition, the ecosystem model includes some diagnostic variables. For example, phytoplankton carbon biomass (mol N m^{-3}) is converted into mol C m^{-3} according to the Redfield ratio (C:N=6.625). Correspondingly, the ratio between phytoplankton biomass and chlorophyll, which is called the C:Chl ratio, is used to calculate chlorophyll concentrations (Wang et al., 2009, 2015). The ratio between phytoplankton biomass and chlorophyll (C:Chl) depends on light, temperature and nutrients (nitrate and iron), whose fields are calculated from the ecosystem model. So, the ocean ecosystem model produces Chl concentration, which is then used to calculate a penetration depth (H_p; Zhang, 2015), representing the Chl effect on the incoming solar radiation in the upper ocean, which exerts a direct influence on the thermodynamics in the upper ocean, which then induces an indirect effect on the dynamics (Zhang et al., 2019b). On the TIW side, TIW-induced Chl signals can also be extracted using the zonal high-passed filter as used in deriving SST_{TIW} signals. Similarly, Chl can be also explicitly separated into three parts, written as: $Chl=Chl_{clim}+Chl_{inter}+Chl_{TIW}$, in which Chl_{clim} is its seasonally-varying climatological field, Chl_{inter} is interannual anomalies, and Chl_{TIW} is TIW-scale perturbations, respectively. The Chl effects on ocean simulations can be taken into account or not in the model experiment. For instance, the Chl effects induced by Chl_{inter} or Chl_{TIW} can be purposely excluded in sensitivity experiments when accounting for their contributions to bio-heating in the temperature equation of the ocean model. As such, the Chl_{inter} or Chl_{TIW} effects can be quantified from sensitivity experiments using the HCM AOPB.

The coupling among these different components in the HCM AOPB is schematically illustrated in Figure 1. For example, atmospheric statistical models are used to calculate interannual anomalies of τ and FWF (i. e., τ_{inter} and FWF_{inter}) from SST_{inter}, and the τ_{TIW} part from SST_{TIW}, respectively. These interannual anomalies are then added onto their prescribed corresponding climatological fields to force the OGCM. The total Chl field is calculated from the ocean ecosystem model; its interannual anomaly part (Chl_{inter}) is depicted relative to its climatological part (Chl_{clim}). On the TIW side, the zonal high-pass filter is applied to daily total SST and Chl fields to explicitly extract TIW signals in the ocean. The SST_{TIW} field is then used to calculate the TIW-induced surface wind stress perturbations (τ_{TIW}) from the constructed empirical τ_{TIW} model, with the SST_{TIW}-τ_{TIW} interaction being explicitly included in the HCM AOPB. Using anomaly coupling method, the atmosphere and ocean are coupled to each other. The empirical response models are used to determine the τ_{inter} and τ_{TIW} parts, which are combined with τ_{clim} to force the OGCM, which, in turn, gives rise to total SST fields; then, SST_{inter} and SST_{TIW} can be obtained correspondingly. The τ_{inter}, τ_{TIW} and SST_{TIW} fields are updated every day in coupled modeling using the SST fields from the OGCM.

The model spin-up and time integration procedures are described in Zhang et al. (2019a). For example, the World Ocean Atlas (WOA01) temperature and salinity fields are used to initiate the OGCM, which is integrated for 20 years using prescribed atmospheric climatological forcing fields; the outcome of this OGCM spinup integration serves as initial conditions in the control and sensitivity experiments for bio-climate coupling studies, respectively. A control experiment is then run for 30 years using the coupled model, in which the evolution is determined solely by the coupled interactions in the system. As shown in Zhang et al. (2018,

2019a), this HCM AOPB can well depict interannual variations associated with ENSO. The end of this 30-year coupled run is arbitrarily denoted as model year 2301. Started from the end of the 30-year control run, the Chl effect-related sensitivity experiments using the HCM AOPB are performed from model year 2301 to model year 2338.

2.2 Experimental design

The HCM AOPB is adopted to represent bio-climate coupling in the tropical Pacific. It turns out that this HCM is able to depict interannual variability associated with ENSO and TIWs quite well (Tian et al., 2018; Zhang et al., 2018). As a model variable estimated from the ocean ecosystem model, for example, Chl exhibits pronounced interannual and TIW signals in the tropical Pacific, which can be explicitly calculated from the HCM AOPB. Explicitly, Chl can be separated into three parts, written as: Chl=Chl_{clim}+Chl_{inter}+Chl_{TIW}. Correspondingly, the Chl-SST feedback at TIW scales can be separately and explicitly included or not in sensitivity experiments.

We perform sensitivity experiments using the HCM AOPB (Figure 2) to illustrate individual or collective effects on ENSO induced by Chl perturbations at interannual and TIW scales (i.e., Chl_{inter} and Chl_{TIW}). The Chl_{inter} and Chl_{TIW} effects on the penetrative solar radiation can be purposely turned on or off in sensitivity experiments. In the control run, which is denoted as Chl_{clim}+Chl_{inter}+Chl_{TIW}, Chl_{inter} and Chl_{TIW} effects both are fully represented in the HCM AOPB, whereas in sensitivity runs, their corresponding effects, individually or collectively, can be alternatively included at interannual and TIW scales, respectively. For example, Chl_{clim}+Chl_{inter} is denoted as a run, in which the Chl_{TIW} signal is explicitly extracted from daily Chl field and its effect on penetrative solar radiation is purposely removed at each time steps in the model integration. Chl_{clim}+Chl_{TIW} is denoted as a run, in which the Chl_{TIW} effect is retained but the Chl_{inter} effect is not taken into account. Chl_{clim} is denoted as a run, in which both the Chl_{TIW} and Chl_{inter} effects are removed. A comparison between the control run and Chl_{clim}+Chl_{TIW} allows to characterize the modulating effect on ENSO induced by Chl_{inter} (i.e. interannual Chl feedback); a comparison between Chl_{clim}+Chl_{inter}+Chl_{TIW} and Chl_{clim}+Chl_{inter} reveals the modulating effect on ENSO induced by Chl_{TIW} (i.e. TIW Chl feedback). Also, a comparison between Chl_{clim}+Chl_{TIW} and Chl_{clim} can reveal the Chl_{TIW} effect on ENSO (i.e. TIW Chl feedback); similarly, a comparison between Chl_{clim}+Chl_{inter} and Chl_{clim} indicates the Chl_{inter} effect on ENSO (i.e. interannual Chl feedback). Comparisons among all these control and sensitivity experiments can be made to reveal the Chl effects on ENSO at interannual and TIW scales, respectively. As such, the individual or combined effects induced by Chl can be assessed in a clean way using the unified modeling framework, which represents the interactions between physical and biogeochemical processes at large and TIW scales, respectively.

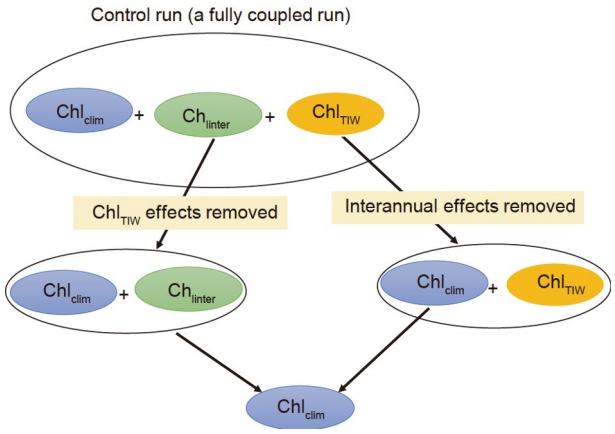

Figure 2 A diagram showing experiments performed in this study. A control run (denoted as Chl_{clim}+Chl_{inter}+Chl_{TIW}) is performed, in which ocean chlorophyll (Chl) is fully represented in the coupled model. The simulated total Chl field can be separated into three parts, written as Chl=Chl_{clim}+Chl_{inter}+Chl_{TIW}, in which Chl_{clim} is its climatological field determined from the long-term run, Chl_{inter} is the corresponding interannual anomalies, and Chl_{TIW} is TIW-induced Chl perturbations (which can be extracted from daily Chl field using a zonal-high-passed filter). Various sensitivity experiments are performed, in which the Chl_{inter} and Chl_{TIW} effects can be turned off based on the control run when accounting for the Chl effects on penetrative solar radiation in the upper ocean.

2.3 Observational and reanalysis data used

We use various observed and reanalysis datasets to specify climatological fields and to construct the statistical models for τ_{inter}, FWF_{inter}, and τ_{TIW}, respectively. Also, some related observations are extensively used to validate model simulations. These data include monthly mean fields of SST from Reynolds et al. (2002), wind stress from the NCEP-NCAR reanalysis, precipitation (P) from the Global Precipitation and Climatology Project (GPCP; Adler et al., 2003), and evaporation (E) from the Objectively Analyzed Air-Sea Fluxes (OAFlux; Yu and Weller, 2007), respectively. Then, FWF fields are derived from P and E data over the period 1979–2008 (the FWF field is positive when there is a net FWF flux from the atmosphere into the ocean). In addition, surface chlorophyll datasets from 1998 to 2016 are available from the GlobColour project, offering a merged level-3 ocean color product by including the SeaWIFS, MODIS, MERIS and VIIRS sensors, respectively (Maritorena and Siegel, 2005). In addition, daily satellite data are used to construct the τ_{TIW} model over the eastern tropical Pacific (Zhang and Busalacchi, 2009a).

Figure 3 presents an example for SST and ocean Chl from satellite observations in the tropical Pacific. TIW signals are clearly evident in the eastern tropical Pacific, with a well-defined trough-ridge structure for SST and Chl. For con-

venience, we refer to a warm SST zone as a TIW ridge, which is accompanied with low Chl concentration. In contrast, a cold SST zone is referred to as a TIW trough, which is accompanied with high Chl concentration. As demonstrated before (e.g., Kessler et al., 1998), TIWs play an important role in the heat balance in the eastern equatorial Pacific. For example, the TIW ridge presents an effective way to transport warm waters from the off-equatorial warm pool region onto the equator, whereas the TIW trough acts to transport cold equatorial waters out of the cold tongue. So, the stronger the TIWs, the more warm waters are transported into the equator, leading to a weakening of the cold tongue in the eastern equatorial Pacific. As such, if TIW intensity is reduced for some reasons, SST in the cold tongue becomes lower.

A schematic diagram is shown in Figure 4 for the structure of TIW-induced SST and Chl fields and their effects on the heat transport in the tropical Pacific. TIWs act to induce a well-defined wavy pattern of SST and Chl: a falling Chl concentration zone is associated with a warm SST perturbation in the TIW ridge region, whereas a rising Chl concentration zone is associated with a cold SST perturbation in the TIW trough region. TIW-scale Chl perturbations can induce bio-heating effects on SSTs in the cold tongue (Tian et al., 2018). In the low Chl region, for example, the negative Chl_{TIW} perturbation causes a deeper penetration of solar radiation, with a less direct bio-heating in the ML (i. e., a corresponding colder SST), which causes a positive density perturbation in the ML. The increased density in the ML ($\delta_{Chl}\_\rho_{TIW}'>0$; here we denote the Chl_{TIW}-induced difference in ρ_{TIW}' as $\delta_{Chl}\_\rho_{TIW}'$, which is differentiated from the TIW-induced total perturbation to density that is denoted as ρ_{TIW}') and decreased one at subsurface de-stabilize the stratification in the upper ocean; this acts to enhance vertical mixing and the entrainment of subsurface cold waters into the ML ($\delta_{Chl}\_w_{TIW}'>0$; here we denote the Chl_{TIW}-induced difference in w_{TIW}' as $\delta_{Chl}\_w_{TIW}'$, which is differentiated from the TIW-induced total perturbation to vertical velocity (w′) that is denoted as w_{TIW}'). Thus, the Chl_{TIW}-induced density perturbations ($\delta_{Chl}\_\rho_{TIW}'$) and the entrainment perturbations ($\delta_{Chl}\_w_{TIW}'$) in the low Chl region are positively correlated. As such, the conversion from the eddy potential energy to kinetic energy (EKE) is reduced (that is, $-\delta_{Chl}\_\rho_{TIW}'\times\delta_{Chl}\_w_{TIW}'<0$; Tian et al., 2018) and TIW intensity is thus decreased.

In the TIW trough region, on the other hand, a rising Chl perturbation leads to a less penetration of solar radiation in the ML, with a more bio-heating and a negative density perturbation ($\delta_{Chl}\_\rho_{TIW}'<0$), which acts to stabilize the upper ocean, leading to weakened vertical mixing and less entrainment of subsurface cold waters into the ML ($\delta_{Chl}\_w_{TIW}'$

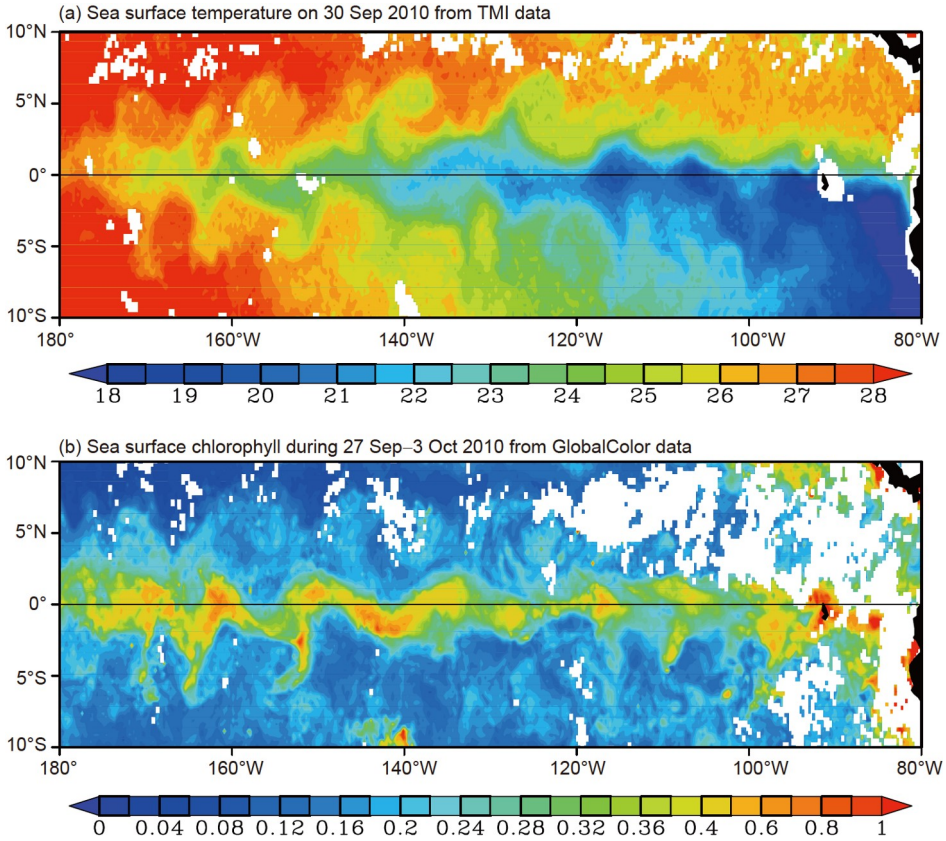

Figure 3 Snapshots for sea surface temperature (SST) on 30 September 2010 and ocean chlorophyll (Chl) during 27 September to 3 October 2010 that are obtained from satellite observations.

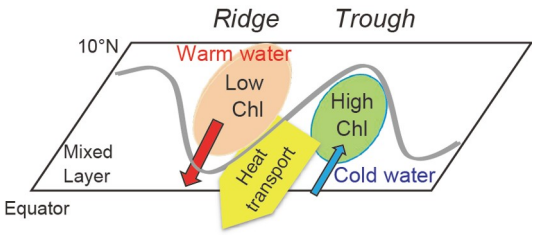

Figure 4 A schematic diagram showing the ridge-trough structure of SST and Chl associated with TIWs in the eastern tropical Pacific. Correspondingly, TIWs play an important role in the heat balance in the cold tongue through the transports of off-equatorial warm waters to the equator.

<0). The conversion from the eddy potential energy to EKE is also decreased ($-\delta_{Chl\_}\rho_{TIW}'\times\delta_{Chl\_}w_{TIW}'<0$) and TIW intensity is still reduced as in the TIW ridge region. Note that a striking feature emerges in the both TIW ridge and trough regions: the Chl-induced bio-heating effects cause a weakening of TIWs themselves. Correspondingly, the weakened TIWs lead to a reduced equatorward transport of the warm waters from the off-equatorial region onto the equator, causing a less warming effect on the cold tongue in the eastern equatorial Pacific. These Chl_{TIW}–induced ocean processes exert an influence on SST in such a way that the SST in the cold tongue is decreased. Therefore, the Chl_{TIW} effects can have a feedback onto SST and thus ENSO. These effects will be tested using sensitivity experiments based on the HCM AOPB as follows.

3. The modulating effects on ENSO

We analyze results from the HCM AOPB-based simulations with different representations of Chl_{inter} and Chl_{TIW} effects. Figures 5–8 illustrate some outcomes of interest from the control run and various sensitivity experiments, including SST fields along the equator (Figure 5), the commonly used Niño3.4 SST index to quantify the major time scales of ENSO events (Figure 6). The effects are quantitatively compared with each other in Table 1 in terms of the standard deviations of the Niño3.4 SST index, which are intended to represent the amplitude of interannual variability associated with ENSO events; large values in Table 1 are interpreted as amplified ENSO cycles. There are noticeable changes in the amplitude of ENSO associated with the Chl effects at interannual and TIW scales. As demonstrated from our previous HCM AOPB-based modeling studies (e.g., Zhang, 2015) and the comparisons with corresponding observations, this model can adequately depict the mean ocean physical and biogeochemical states in the tropical Pacific. Also, the model can capture ENSO cycles quite well, indicating that the main coupled ocean-atmosphere processes should be adequately represented in a balanced way. For example, the HCM AOPB can produce pronounced ENSO events, with an approximate four-year interannual oscillation period (Figure 6).

3.1 The total Chl effects in the control run

We refer to the $Chl_{clim}+Chl_{inter}+Chl_{TIW}$ experiment as a control run, in which the Chl effects are fully represented on ocean simulations. An example for simulated Chl field in the control run is shown in Figures 7 and 8. Chl exhibits clear variations at interannual and TIW scales. At interannual scales, anomaly fields of SST (Figure 5a) and Chl (Figure 7b) exhibit well-defined patterns, with their coherent relationships. For instance, a warm SST anomaly is seen in the central-eastern equatorial Pacific during El Niño (Figure 5a), which is accompanied with a low Chl concentration in the western-central equatorial region (Figures 7a, 7b). At TIW scales, TIW-induced perturbations are evident in the eastern tropical Pacific. Examples for daily total fields of SST and Chl are shown in Figure 8; their wavy patterns can be clearly seen in the eastern equatorial Pacific (Figure 8). In the TIW ridge region, for example, a warm SST zone is accompanied with low Chl concentration (Figure 8a, 8c). In a TIW trough region, in contrast, a cold SST zone is accompanied with high Chl concentration. To highlight TIW-scale signals of SST and Chl, we apply a zonal high-passed

Table 1 The standard deviation (STD; unit: °C) and period of the Niño3.4 index (unit: year) simulated in the related sensitivity experiments [a)]

Experiments	Niño3.4 SSTA STD (the relative change ratio)	Oscillation periods (year)
$Chl_{clim}+Chl_{inter}+Chl_{TIW}$ (the control run)	0.79	4.24
$Chl_{clim}+Chl_{inter}$	0.62 (–21%)	4.14
$Chl_{clim}+Chl_{TIW}$	1.06 (+31%)	4.14
Chl_{clim}	0.98 (+19%)	4.18

a) Also shown are the STD change ratio in the three sensitivity experiments relative to the control run. In addition, the Chl_{TIW} effect can be quantatively assessed in two way: one is the change in the STD from the $Chl_{clim}+Chl_{inter}$ run to the $Chl_{clim}+Chl_{inter}+Chl_{TIW}$ run (here the Chl_{TIW} effect causes an increase by 27%); the other is the change from the Chl_{clim} run to the $Chl_{clim}+Chl_{TIW}$ run (an increase by 8%). Also, the Chl_{inter}-induced effect can be assessed in two way: one is the change from the $Chl_{clim}+Chl_{TIW}$ run to the $Chl_{clim}+Chl_{inter}+Chl_{TIW}$ run (a decrease by 25%); the other is the change from the Chl_{clim} run to the $Chl_{clim}+Chl_{inter}$ run (a decrease by 37%), respectively.

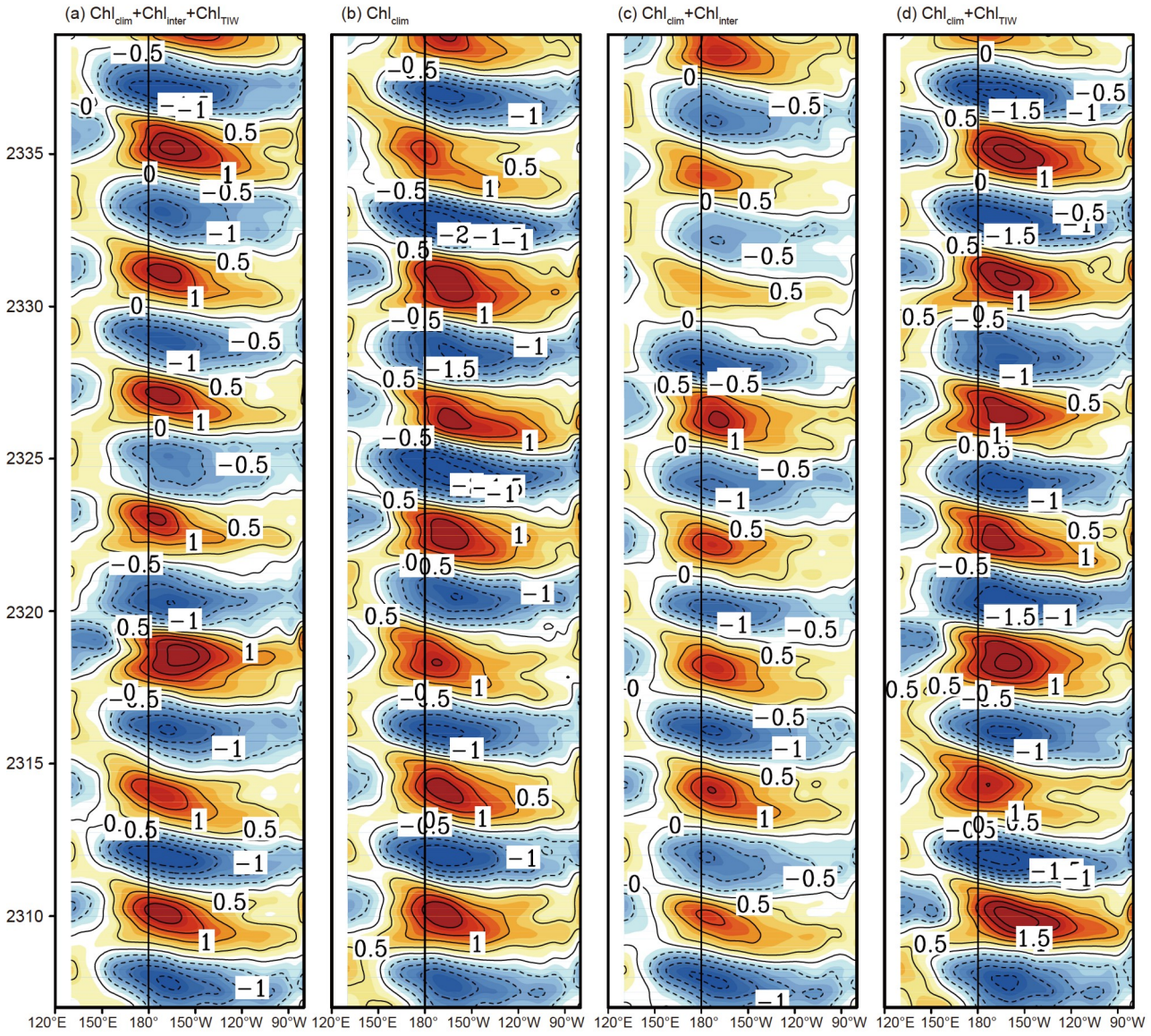

Figure 5 Interannual SST anomalies along the equator simulated in Chl$_{clim}$+Chl$_{inter}$+Chl$_{TIW}$ (a), Chl$_{clim}$ (b), Chl$_{clim}$+Chl$_{inter}$ (c), and Chl$_{clim}$+Chl$_{TIW}$ (d), respectively. The contour interval is 0.5 °C.

filter to their daily fields: a 12° zonal moving average is first performed to obtain a corresponding large-scale background field, which is then subtracted from the original field to extract TIW perturbation fields. More clear details are shown in Figure 9 for TIW-scale perturbations simulated from the control run (Chl$_{clim}$+Chl$_{inter}$+Chl$_{TIW}$), including SST, surface Chl, and vertical velocity at the base of the ML (denoted as w_{TIW}'). As shown in Figure 9a and Figure 9b, the TIW-scale warm (cold) SST perturbations in the ridge (trough) regions of the eastern tropical Pacific are accompanied with low (high) Chl concentration. In addition, negative vertical velocity perturbations (w_{TIW}') near (120°W, 1°N) at the base of the ML are seen in Figure 9c, an area where large warm SST perturbations and negative Chl perturbations are located.

Thus, there coexist Chl perturbations at interannual and TIW scales in the tropical Pacific during ENSO cycles. An example is showed in Figure 10 for the total Chl field which is separated into its climatological, interannual and TIW components, respectively. The relationships between SST and Chl at interannual and TIW scales (indicating their intensities) are illustrated in Figure 11; the SST and Chl fields referred to here are defined in different regions because these fields exhibit their strongest interannual signals in the corresponding regions. At interannual and TIW scales, SST and Chl perturbations are negatively correlated with each other. As has been previously demonstrated, the Chl$_{inter}$ and Chl$_{TIW}$ perturbations can individually modulate ENSO (Tian et al., 2019; Zhang et al., 2019a). Here, as a whole, the Chl effects can be seen by comparing simulations in the control run

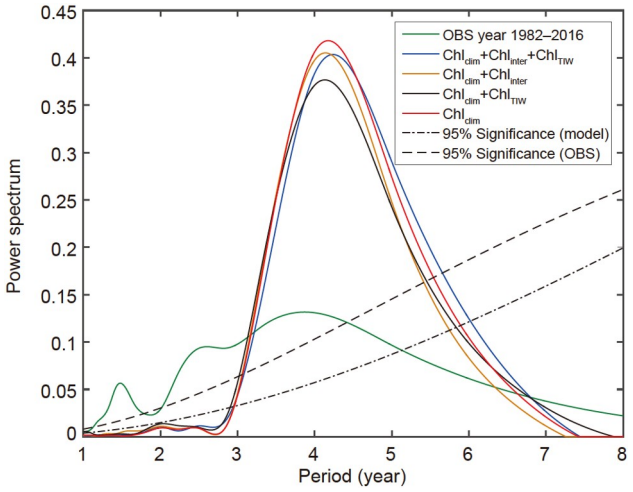

Figure 6 Wavelet power spectra for the Niño3.4 SST anomalies calculated from the Chl$_{clim}$+Chl$_{inter}$+Chl$_{TIW}$ (blue line), Chl$_{clim}$+Chl$_{inter}$ (orange line), Chl$_{clim}$+Chl$_{TIW}$ (black line) and Chl$_{clim}$ (red line), as well as from SST observations. The dot-dashed line is the 95% significance level for these simulations, assuming a white noise process.

(Figure 5a) with those in the Chl$_{clim}$ run (Figure 5b). It is evident that interannual SST anomalies and ENSO amplitude in the control run are obviously reduced compared with those in the Chl$_{clim}$ run, in which both interannual and TIW Chl effects are not represented. A quantitative comparison between the SST simulations is given in Table 1. The standard deviation of the Niño3.4 SST anomalies is 0.79 °C in the control run and is 0.98 °C in the Chl$_{clim}$ run; in terms of the Niño3.4 SST variability, these values represent a decrease of approximately 19% in the control run relative to the Chl$_{clim}$ run. As demonstrated in our previous modeling studies (e.g., Zhang et al., 2012; Zhang, 2015; Tian et al., 2018), Chl-induced heating acts to have dynamic effects on ocean density, stratification and vertical mixing in the upper ocean; these processes then exert an influence on SST, a field that directly forces changes in the atmosphere, which can affect large-scale ocean-atmosphere interactions and thus ENSO.

Note that obvious biases exist in the simulated ENSO from the control run as compared to observations. For example, the simulated ENSO is quite regular, which can be attributed to the fact that atmospheric stochastic forcing is not included in the HCM AOPB. In addition, the spatial pattern of SST interannual variability simulated from the HCM looks like the central Pacific (CP) type of El Niño (Yu and Kim, 2010), whereas the observed SST variability shows the diversity of El Niño events. So, the spatial patterns of SST interannual

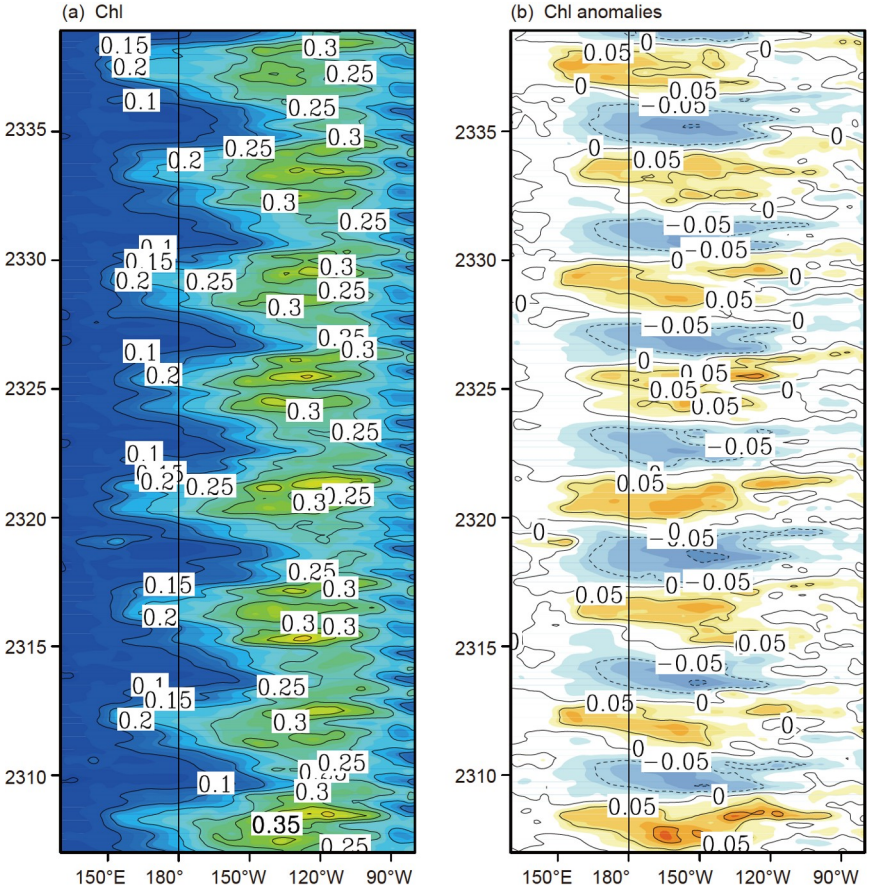

Figure 7 Longitude-time sections along the equator for total Chl field (a) and its interannual anomalies (b) simulated from the control run. The contour interval is 0.05 mg m^{-3}.

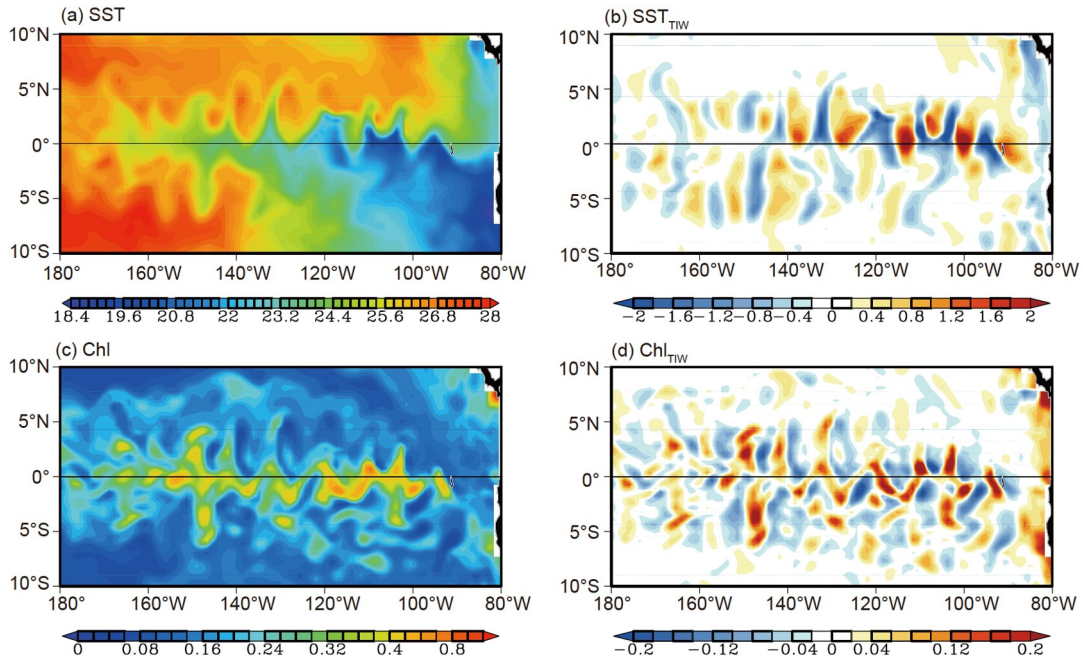

Figure 8 Snapshots for simulated fields in the mixed layer from the control run on 30 September 2307: (a) SST, (b) SST_{TIW}, (c) Chl, and (d) Chl_{TIW}. The units are °C in (a) and (b), and mg m^{-3} in (c) and (d).

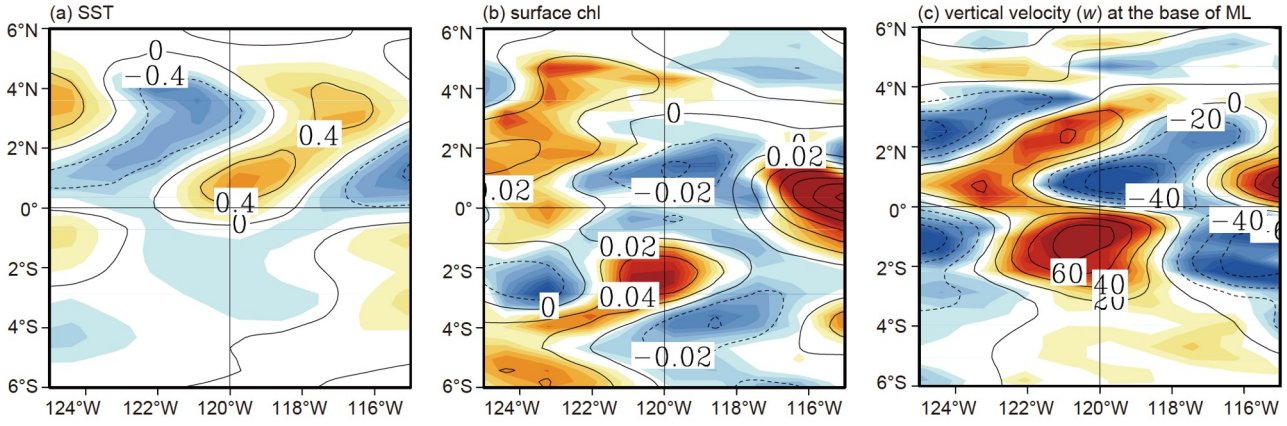

Figure 9 Snapshots for TIW-scale perturbations simulated from the control run (Chl_{clim}+Chl_{inter}+Chl_{TIW}) on 1st January 2310: (a) SST, (c) surface Chl, and (c) vertical velocity at the base of the ML. The units are °C, mg m^{-3}, and cm day^{-1} in (a), (b) and (c), respectively.

variability in the model simulations are somehow distinct from what is observed.

Because interannual and TIW-scale Chl perturbations co-exist in the control run with their effects being mixed together in the simulations, it is difficult to reveal their individual roles played in the ENSO modulations. More sensitivity experiments are thus performed in the following subsections, in which Chl_{inter} and Chl_{TIW} effects can be alternatively taken into account or not in modeling experiments so that their individual effects on ENSO can be illustrated and quantified in a clear way.

3.2 The Chl_{inter} effect

Referring to the Chl_{clim} run, the Chl_{clim}+Chl_{inter} run is a run in which the Chl_{inter} effect is included; their comparisons can illustrate the Chl_{inter} effect. Also, referring to the Chl_{clim}+Chl_{TIW} run, the control run (Chl_{clim}+Chl_{inter}+Chl_{TIW}) is a run in which the Chl_{inter} effect is included; their comparisons can illustrate the Chl_{inter} effect as well. Examples for SST interannual anomalies simulated in these runs are shown in Figures 5 and 6. As seen in the Chl_{clim}+Chl_{inter} run and the control run, interannual Chl variability can be well depicted during ENSO cycles (e. g., Figure 7), which can thus induce feedback effects onto ENSO.

Figure 12 illustrates interannual anomalies in January 2310 during an El Niño event, which is derived from the Chl_{clim}+Chl_{inter}+Chl_{TIW} run (the control run) and the Chl_{clim}+Chl_{TIW} run for SST, surface density (ρ_{surf}) and their differences. The

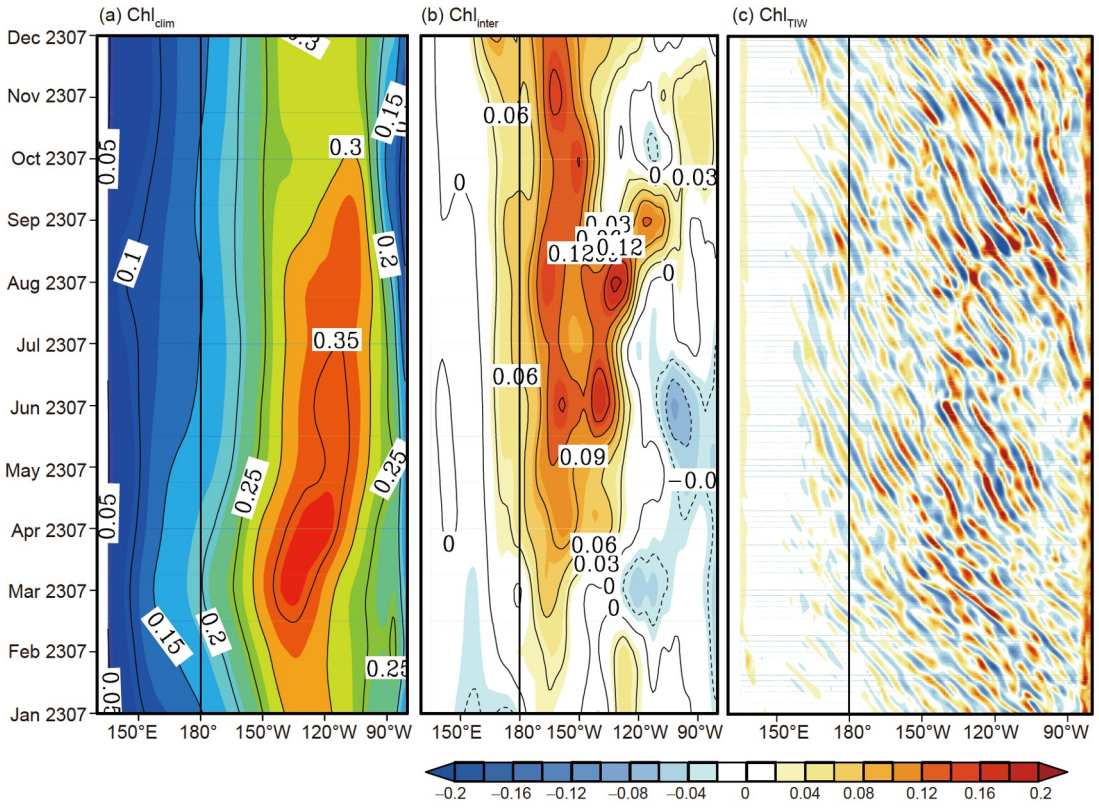

Figure 10 Longitude-time sections along the equator for the climatological chlorophyll field (a), interannual Chl anomalies (b) and TIW-scale Chl perturbations (c) in 2307 from the control run. The total chlorophyll field can be separated into Chl_{clim}, Chl_{inter}, and Chl_{TIW} parts, respectively. The contour intervals are 0.05 mg m^{-3} in (a), 0.03 mg m^{-3} in (b), and 0.02 mg m^{-3} in (c).

processes involved in the Chl_{inter} feedback have been illustrated previously in Zhang et al. (2019a); a corresponding negative feedback loop can be traced in association with the Chl_{inter} effects on the penetrative solar radiation in the upper ocean (Figure 13). During El Niño events, for example, warm SST anomalies in the central-eastern equatorial Pacific are accompanied with a drop in Chl concentration in the western-central equatorial Pacific, which causes a deeper penetration of sunlight in the upper ocean, with bio-heating less in the ML but more at subsurface. This correspondingly gives rise to a vertical differential heating between the ML and subsurface layers, which acts to destabilize the upper ocean, with the enhanced vertical mixing and entrainment of subsurface waters into the ML. Thus, the negative Chl anomalies during El Niño act to modulate ocean processes in such a way that El Niño events are reduced by the indirectly induced dynamical influence on SST. The processes and effects induced during La Niña are opposite to those during El Niño, but with opposite sense. During La Niña events, for instance, a rise in Chl concentration is accompanied with cold SST anomalies; the rising Chl concentration in the western-central equatorial Pacific causes the incoming solar radiation to be trapped more within the ML but penetrated less throughout the bottom of the ML (less bio-heating in the subsurface layers), which stabilizes the stratification and weakens vertical mixing in the upper ocean. These processes act to warm up the sea surface and increase SST so that La Niña is weakened. Therefore, the interannually varying Chl effects give rise to a negative feedback onto ENSO, acting to reduce amplitude of El Niño and La Niña events, respectively.

Quantitatively, compared with the Chl_{clim}+Chl_{TIW} run in Figure 5d (the standard deviation is 1.06 °C), the ENSO amplitude is reduced in the control run (the standard deviation is 0.79 °C), indicating a reduction in the standard deviation by approximately 34%. So, the interannual Chl effect is characterized by a negative feedback onto ENSO. Also, relative the Chl_{clim} run (Figure 5b), ENSO amplitude is reduced in the Chl_{clim}+Chl_{inter} run (Figure 5c) when interannually varying Chl feedback is included; the standard deviation of the Niño3.4 SST anomalies is 0.98 °C in the Chl_{clim} run and is reduced to 0.62 °C in the Chl_{clim}+Chl_{inter} run (Table 1), indicating a reduction by 30%.

3.3 The Chl_{TIW} effect

Next, move onto the Chl effect at TIW scales. Referring to the Chl_{clim} run (Figure 5b), the Chl_{clim}+Chl_{TIW} run is a run in which the Chl_{TIW} effect is taken into account (Figure 5d); their comparisons can illustrate the Chl_{TIW} effect. Also, re-

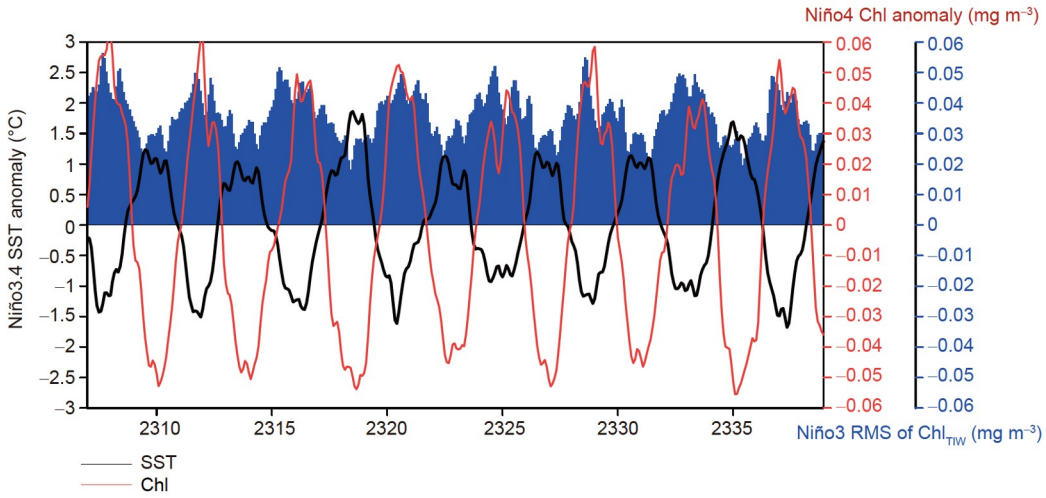

Figure 11 Interannual anomalies of sea surface temperature (SST) in the Niño3.4 region (black line) and chlorophyll in the Niño 4 region (red line), and the root mean square (RMS) of Chl_{TIW} in the Niño3 region (blue bars) calculated from the control run during 2307–2338. The units are °C for SST and mg m^{-3} for Chl.

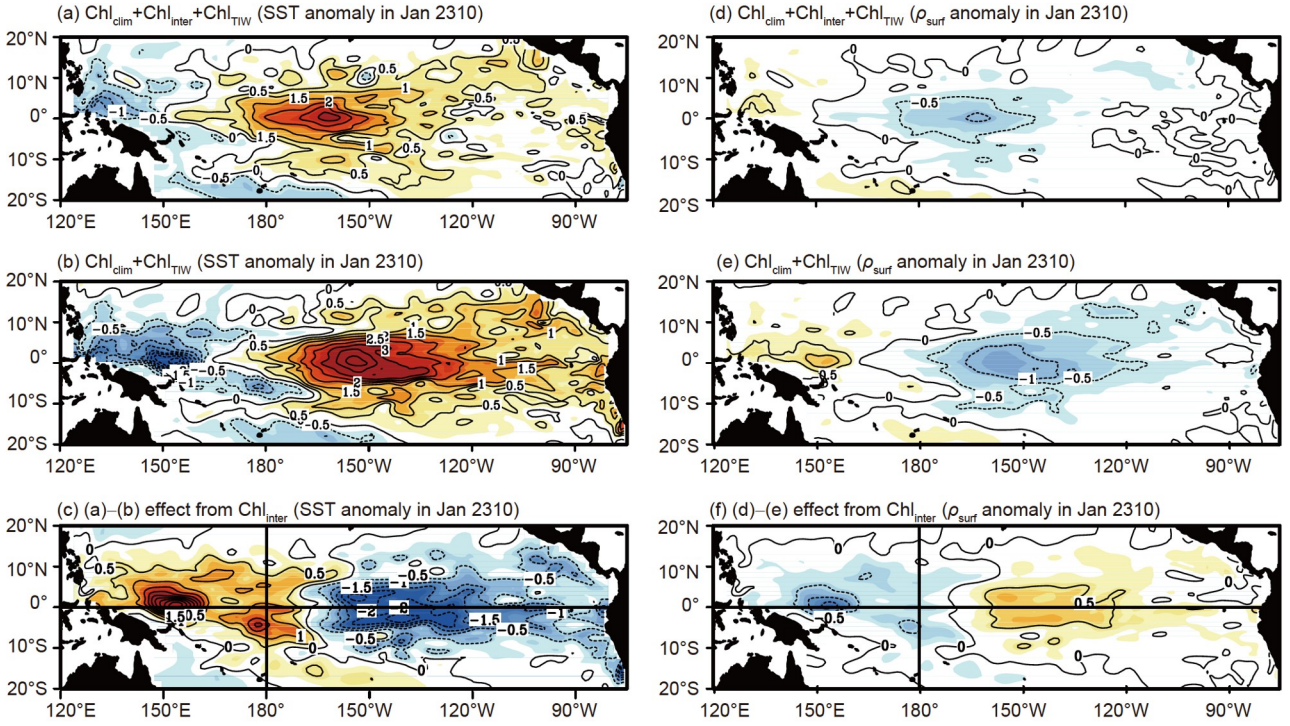

Figure 12 Interannual anomalies in January 2310 during an El Niño event derived from the Chl_{clim}+Chl_{inter}+Chl_{TIW} run (the control run) and the Chl_{clim} +Chl_{TIW} run: SST in (a) and (b), and surface density (ρ_{surf}) in (d) and (e); (c) and (f) are respectively for the SST and ρ_{surf} differences between the runs with and without interannual Chl effect. The contour intervals are 0.5 °C for SST and 0.5 kg m^{-3} for ρ_{surf}, respectively.

ferring to the Chl_{clim}+Chl_{inter} run (Figure 5c), the Chl_{TIW} effect is retained in the control run (Chl_{clim}+Chl_{inter}+Chl_{TIW}); their comparisons (Figure 5c and Figure 5a) can illustrate the Chl_{TIW} effect as well. TIW signals are seen in daily SST and Chl fields simulated in these model experiments, with a warm (cold) SST perturbation in the TIW ridge (trough) region being accompanied with a falling (rising) Chl concentration (Figure 8), respectively. The 12° zonal high-passed filter is applied to daily fields of SST and Chl to extract the SST_{TIW} and Chl_{TIW} signals (e. g., Figure 8). TIW-induced negative (positive) Chl perturbations are seen in the TIW ridge (trough) region, which can have effects on ENSO (Tian et al., 2018). Examples of simulated interannual SST anomalies are shown in Figure 5 and Figure 6 in the related model sensitivity simulations, with the effects being quantified in Table 1. Relative to the Chl_{clim} run (Figure 5b), for

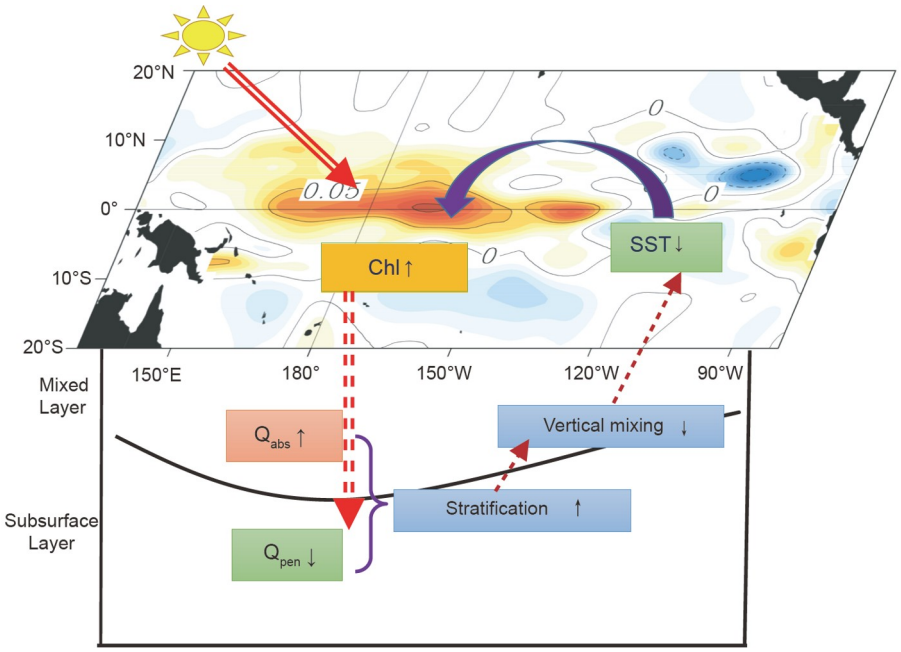

Figure 13 A schematic diagram illustrating processes involved in a negative feedback onto ENSO due to interannual chlorophyll (Chl_{inter}) effect. During La Niña, for example, a cold SST anomaly prevails in the eastern tropical Pacific, accompanied with a positive Chl anomaly in the western-central equatorial Pacific. The positive Chl anomaly leads to solar radiation absorbed more within the mixed layer (an increase in Q_{abs}), and penetrated less out of the bottom of the mixed layer (a decrease in Q_{pen}). The differential heating vertically in the mixed layer and subsurface layers acts to stabilize the stratification and weaken the vertical mixing, which weakens the cold SST anomalies during La Niña. The situation during El Niño is similar to La Niña situation but with opposite sense. Thus, a negative feedback emerges that is induced by the Chl_{inter} effect in the bio-climate system of the tropical Pacific.

instance, the ENSO amplitude is increased in the Chl_{clim} +Chl_{TIW} run (Figure 5d) when the Chl_{TIW} feedback is included; their standard deviations of the Niño3.4 SST anomalies are respectively 0.98 °C and 1.06 °C, which represents an increase by 8%. Compared to the Chl_{clim}+Chl_{inter} run (Figure 5c) which has the standard deviation of 0.62 °C, the ENSO amplitude in the control run is increased (Figure 5a; the standard deviation is 0.79 °C), which represents an increase by 27%. So, TIW-scale Chl perturbations exert an influence on SSTs in the tropical Pacific, which is characterized by an enhancing effect on ENSO.

Figure 14 further illustrates the processes involved in the Chl_{TIW} effects on ENSO (Tian et al., 2018, 2019). TIWs produce pronounced wavy patterns in SST (SST_{TIW}) and chlorophyll (Chl_{TIW}), with their anticorrelation in the eastern tropical Pacific (Figure 9), accompanied with upwelling and downwelling, respectively. A corresponding positive feedback loop can be traced in association with the Chl_{TIW} effect. In the eastern tropical Pacific, a warm (cold) SST_{TIW} perturbation is accompanied with a falling (rising) Chl_{TIW} perturbation in the TIW ridge (trough) regions. In the TIW ridge region with a warm SST_{TIW}-low Chl_{TIW} configuration, for example, solar radiation is absorbed less within the ML (Q_{abs}) but penetrates more into the subsurface layer (Q_{pen}) in the TIW ridge regions. Consequently, the Chl_{TIW} effects cause a positive density perturbation in the ML (i. e., $\delta_{Chl\_}\rho_{TIW}'>0$; here we denote the Chl_{TIW}-induced difference in ρ_{TIW}' as $\delta_{Chl\_}\rho_{TIW}'$, which is differentiated from the total TIW-induced perturbation to density that is denoted as ρ_{TIW}'), with a negative one in the subsurface layers. Thus, the Chl_{TIW} effects act to destabilize the stratification and enhance vertical mixing in the upper ocean and the entrainment of subsurface waters into the ML ($\delta_{Chl\_}w_{TIW}'>0$; here the Chl_{TIW}-induced difference in ρ_{TIW}' is denoted as $\delta_{Chl\_}\rho_{TIW}'$, which is differentiated from the TIW-induced total perturbation to density that is denoted as ρ_{TIW}', being negative in the TIW ridge region as shown in Figure 9c). As such, the effect of the low Chl_{TIW} perturbation directly causes a reduction in the baroclinic conversion term ($-\delta_{Chl\_}\rho_{TIW}'\times\delta_{Chl\_}w_{TIW}'<0$) from the eddy potential energy into the eddy kinetic energy (EKE). That is, the negative values of this term becomes more negative in the low Chl_{TIW} concentration ridge regions in the control run compared with the Chl_{TIW}-filtered run. Thus, there is a decrease in the EKE supply to TIWs due to the Chl_{TIW} effect, leading to a weakening of TIWs. At the same time, the intensity of the warm SST_{TIW} perturbation is also reduced due to the enhanced vertical mixing in the TIW ridge region. The combined effects of these processes act to cause a reduction in TIW intensity in the eastern tropical Pacific.

Similarly, in the TIW trough regions, a cold SST_{TIW} perturbation is accompanied with high Chl_{TIW} concentration and upwelling motion. Here, solar radiation is absorbed more within the ML (Q_{abs}) but penetrates less out of the bottom of ML (Q_{pen}) in the TIW trough regions. The vertical differ-

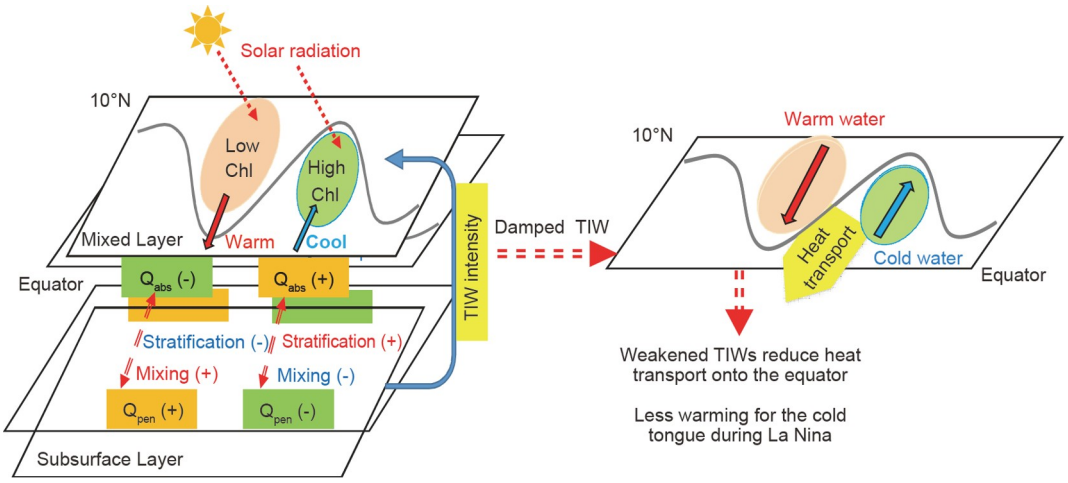

Figure 14 A schematic diagram illustrating processes and direct effects which are induced by TIW-scale chlorophyll (Chl_{TIW}) perturbations and a positive feedback onto ENSO. TIWs produce pronounced wavy patterns in SST (SST_{TIW}) and chlorophyll (Chl_{TIW}). In the TIW ridge (trough) region, a warm (cold) SST_{TIW} perturbation is accompanied with a falling (rising) Chl_{TIW} perturbation. The Chl_{TIW} perturbations act to induce bio-heating effects.

ential bio-heating in the ML and subsurface layers causes a negative density perturbation in the ML (i. e., $\delta_{Chl\_}\rho_{TIW}'<0$) but a positive one in the subsurface layers. Thus, the positive Chl_{TIW} perturbations act to stabilize the stratification and reduce the vertical mixing. Correspondingly, the entrainment of subsurface waters into the ML is decreased (i.e., $\delta_{Chl\_}w_{TIW}'<0$). As such, the Chl_{TIW} effect with high Chl concentration directly causes a reduction in the baroclinic conversion term ($-\delta_{Chl\_}\rho_{TIW}'\times\delta_{Chl\_}w_{TIW}'<0$) from the eddy potential energy into the EKE. That is, this term also becomes more negative in the trough regions with high Chl_{TIW} concentration in the control run relative to the Chl_{TIW}-filtered run. So, the EKE supply to TIWs is decreased due to the high Chl_{TIW} concentration effect, leading to TIWs that are weakened. At the same time, the intensity of the cold SST_{TIW} perturbation is reduced due to the weakened vertical mixing in the TIW trough region. The combined effects of these processes act to modulate TIWs in such a way that TIW intensity is reduced.

In short summary, the Chl_{TIW} perturbations act to induce bio-heating effects as follows. In the TIW ridge region with low Chl concentration, for example, solar radiation is absorbed less within the mixed layer (a decrease in Q_{abs}) but penetrates more into the subsurface layer (an increase in Q_{pen}). Consequently, a positive density perturbation is produced in the mixed layer, with a negative one in the subsurface layers; thus, the stratification is destabilized with enhanced vertical mixing in the upper ocean, leading to an increase in the entrainment of subsurface waters into the mixed layer. As such, the effect with low Chl_{TIW} perturbation directly causes a reduction in the baroclinic conversion term from the eddy potential energy into the eddy kinetic energy (EKE). Thus, the EKE supply to TIWs is reduced due to the effect of low Chl_{TIW} concentration, consequently reducing TIW intensity in the eastern tropical Pacific. Similarly, in the TIW trough region where cold SST_{TIW} perturbation is accompanied with a rising Chl_{TIW} perturbation, solar radiation is absorbed more within the mixed layer (an increase in Q_{abs}) but penetrates less out of the bottom of ML (a decrease in Q_{pen}). The differential heating in the mixed layer and subsurface layers causes a negative density perturbation in the mixed layer but a positive one in the subsurface layers, which acts to stabilize the stratification and reduce the vertical mixing. Correspondingly, the entrainment of subsurface waters into the mixed layer is decreased. As such, the effect with high Chl_{TIW} perturbation directly causes a reduction in the baroclinic conversion term from the eddy potential energy into the eddy kinetic energy. So, the high Chl_{TIW} concentration effect in the TIW ridge region also leads to a decreased EKE supply to TIWs. It is striking that the Chl_{TIW}-induced density and entrainment perturbation fields are positively correlated both in the TIW trough and ridge regions. As such, the EKE and TIW intensities are reduced due to the Chl_{TIW} effects in the eastern tropical Pacific. The weakened TIWs due to the Chl_{TIW} effect act to reduce the meridional heat transport onto the equator and consequently cause a less warming effect on the cold tongue in association with the northern off-equatorial warm waters. As a result, the surface layer cools down more in the eastern equatorial Pacific due to the TIW-induced Chl effects.

It is interesting to note that the Chl_{TIW} effects associated with the warm SST_{TIW}-low Chl_{TIW} and cold SST_{TIW}-high Chl_{TIW} configurations both cause a reduction in the energy conversion term from the EPE to the EKE ($-\delta_{Chl\_}\rho_{TIW}'\times\delta_{Chl\_}w_{TIW}'<0$) so that the Chl_{TIW}-induced effects on $\delta_{Chl\_}\rho_{TIW}'$ and $\delta_{Chl\_}w_{TIW}'$ fields are positively correlated in regions with active TIWs. As such, the EKE and TIW intensities are reduced due to the Chl_{TIW} effects in the eastern

tropical Pacific.

Climatologically, the northern off-equatorial region in the northeastern tropical Pacific is occupied with the warm pool, accompanied with the cold tongue on the equator. As has been previously demonstrated by Kessler et al. (1998), TIWs play an important role in the heat balance of the cold tongue in the eastern equatorial Pacific; the off-equatorial warm waters in the northeastern tropical Pacific are transported equatorward onto the equator, thus warming up the cold tongue.

As demonstrated by the HCM AOPB simulations above, the Chl_{TIW} effects tend to suppress the TIW intensity in the eastern equatorial Pacific, which acts to reduce the meridional heat transport onto the equator due to the weakened transport of the off-equatorial warm waters, consequently leading to a less warming effect on the cold tongue on the equator. As a result, SST cools down more in the eastern equatorial Pacific compared with a case in which the TIW-scale Chl effect is not included. Moreover, note that TIWs tend to be strong during cold seasons and La Niña events, but become weak or do not exist during warm seasons and El Niño events. Then, it is expected that cold SST anomalies during La Niña events are intensified due to the Chl_{TIW} effect in the Chl_{clim}+Chl_{inter}+Chl_{TIW} run compared with the Chl_{clim} +Chl_{inter} run. Further, the intensified cold SST anomalies in the cold tongue due to the Chl_{TIW} effect become even larger through large-scale ocean-atmosphere interactions, making La Niña events stronger. In this sense, the Chl_{TIW} effect acts to have a positive feedback on ENSO events, with the increased ENSO amplitude in the HCM AOPB simulations when the Chl_{TIW} effect is represented.

Note that the ENSO variability is smaller in the control run than in the observation and the Chl-induced impacts on the ENSO period seem minor (Table 1 and Figure 6). In addition, there exist nonlinear interplays among the Chl effects at interannual and TIW scales. For example, the modulated effects on ENSO amplitude in the Chl_{clim}+Chl_{inter}+Chl_{TIW} run is not equal to the combination of the Chl_{clim}+Chl_{inter} run and Chl_{clim}+Chl_{TIW} run (Table 1). Also, in terms of the Chl_{TIW} effect, the Chl_{TIW}-induced difference in the Chl_{clim}+Chl_{inter} +Chl_{TIW} run and Chl_{clim}+Chl_{inter} run is not equal to that in the Chl_{clim}+Chl_{TIW} run and the Chl_{clim} run. In terms of Chl_{inter} effect, the Chl_{inter}-induced difference in the Chl_{clim}+Chl_{inter} +Chl_{TIW} run and Chl_{clim}+Chl_{TIW} run is not equal to that in the Chl_{clim}+Chl_{inter} run and the Chl_{clim} run, respectively. These effects are also quantitatively assessed in Table 1.

4. Conclusions and discussions

Pronounced Chl perturbations are observed to coexist at interannual and TIW scales in the tropical Pacific, acting to not only indicate a response to ENSO but also induce a feedback onto ENSO. In this work, we use a hybrid coupled model (HCM) of the atmosphere and ocean physics-biogeochemistry (AOPB) to study the bio-climate interactions; the HCM AOPB consists of an oceanic general circulation model, an ocean ecosystem model, and statistical atmospheric models for interannual anomalies of wind stress and FWF (τ_{inter} and FWF_{inter}), respectively. In addition, TIW-induced surface wind feedback is also included in the HCM AOPB. The model can well capture chlorophyll (Chl) in the tropical Pacific, which can have a direct modulating effect on the penetrative solar radiation in the upper ocean. Also, the HCM AOPB can adequately depict TIWs and interannual variability, including the Chl_{TIW} and Chl_{inter} signals in the tropical Pacific. Then, the HCM AOPB is used to quantify how ENSO is modulated by Chl-induced bio-effects both at interannual and TIW scales, respectively. To this end, specific sensitivity experiments are performed using the HCM AOPB, in which the Chl_{inter} and Chl_{TIW} effects are taken into account or not, individually or collectively.

It is demonstrated that active bio-climate interactions coexist at interannual and TIW scales in the tropical Pacific. The amplitudes of ENSO can be substantially affected by interannual and TIW-related Chl effects. Individually, interannual Chl anomalies can have a damping effect on ENSO; a negative feedback associated with interannual Chl variability acts to reduce ENSO amplitude and shorten its time scales. In contrast, TIW-scale Chl feedback can have an amplifying effect on ENSO; a positive feedback is associated with TIW-induced Chl perturbations, acting to enhance ENSO amplitude. When these two signals coexist in the tropical Pacific, their collective effects emerge on the penetrative solar radiation in the upper ocean. The damping effects on ENSO due to interanual Chl variability tend to counteract the TIW-induced amplifying effects, leading to their combined net effects on ENSO that can differ from those induced individually. Because there exist the compensated effects of TIW and interannual Chl perturbations, ENSO amplitude can be modulated to increase or decrease, sensitively depending on the relative dominance of these two effects represented in a model. It is the relative dominance of the bio-effects induced by TIW or interannual Chl perturbations that determines how ENSO is actually modulated in model simulations.

In association with Chl_{inter} and Chl_{TIW} perturbations, corresponding bio-feedback effects can be illustrated on dynamical ocean processes in the upper ocean. In terms of interannual bio-feedback, for example, an increase in Chl concentration during La Niña over the western-central equatorial Pacific causes a shallower penetration of solar radiation, with more bio-heating within the ML but less in the subsurface layers; the produced vertical differential density field between the ML and subsurface layers enhances the stratification with weakened vertical mixing. These

processes act to reduce the negative SST anomalies during La Niña, indicating a negative feedback. In terms of TIW-scale effects, the TIW ridge region with high SST is characterized by a falling Chl concentration, which causes a deeper penetration of solar radiation, with a less bio-heating and a positive density perturbation in the ML. The negative Chl_{TIW} perturbations act to increase water density in the ML ($-\delta_{Chl\_}\rho_{TIW}'>0$) and enhance the entrainment of subsurface cold waters into the ML ($\delta_{Chl\_}w_{TIW}'>0$), which reduces the energy conversion from the eddy potential energy to the kinetic energy ($-\delta_{Chl\_}\rho_{TIW}'\cdot\delta_{Chl\_}w_{TIW}'<0$), with TIW intensity thus being decreased. The situation in the TIW trough region with a rising Chl perturbation is similar. The conversion from the eddy potential energy to the kinetic energy due to the Chl_{TIW} effects is also reduced, leading to TIW intensity that is decreased as well. The weakened TIWs lead to a reduced equatorward transport of the warm waters from the off-equatorial warm pool region onto the equator, leading to a less warming effect on the cold tongue in the eastern equatorial Pacific. These Chl_{TIW}-induced ocean processes exert an influence on SST in such a way that SST is reduced in the cold tongue. That is, Chl_{TIW} perturbations in the eastern tropical Pacific have amplifying effects on ENSO.

Thus, the ways Chl effects are represented in models can be a clear source for model biases and uncertainties in ENSO simulations. As demonstrated from this study, ENSO modulations are sensitively dependent on the ways Chl effects are represented in the model, showing a scale-dependence at interannual and TIW scales. As such, if the Chl effects are not adequately represented, biases in ENSO simulations can be produced. In large-scale climate models that do not resolve TIW-scale Chl effects, for example, overestimated biases in ENSO amplitude can be produced (Zhang, 2015; Kang et al., 2017). Thus, it is necessary to care about the modulating effects on ENSO simulations induced both by TIW and interannual Chl effects. In this study, Chl effects are quantified at interannual and TIW scales, providing a new insight into the complexity of ENSO modulations induced by ocean biogeochemistry in the tropical Pacific.

TIWs are important small-scale phenomena in the eastern tropical Pacific, impacting heat transport onto the equator in the cold tongue. This modeling study indicates that TIWs play a role not only through physical processes, but also through ocean biogeochemistry processes. As demonstrated, TIWs clearly impact the ocean ecosystem in the tropical Pacific as indicated in Chl, which affects the penetration of solar radiation at TIW scales. Chl_{TIW}-induced bio-heating exerts effects on SST in the cold tongue of the tropical Pacific. In particular, TIW-scale perturbations can also have effects on ENSO, which is counteracting to those of interannual Chl variability. Thus, there exist apparent interplays that are involved between physical and biogeochemistry processes due to Chl-induced effects at interannual and TIW scales. Individually, ENSO amplitude can be modulated to decrease (increase) with the Chl_{inter} (Chl_{TIW})-induced effects; collectively, whether ENSO amplitude can be modulated to increase or decrease is determined by their combined net effects. Furthermore, interactions between physical and biogeochemistry processes exist at interannual and TIW scales. For instance, TIWs undergo fluctuations on seasonal and interannual scales in the tropical Pacific, which give rise to complicated interplays between TIW and interannual Chl effects. Right now, these complicated interplays and effects on ENSO through the ocean ecosystems in the tropical Pacific (as indicated by Chl concentration) at interannual and TIW scales are still not clear and need to be addressed with more focused modeling experiments. The developed HCM APOB in this paper can be used to understand the influence pathways due to the Chl-induced heating on ENSO. Further studies are clearly needed to understand the interactions between physical and biogeochemistry processes in the tropical Pacific at interannual scales and TIW scales, respectively.

Note that obvious biases exist in our modeling framework adopted in this study. For example, one discrepancy in the HCM simulations is that the ENSO-related variability is too regular; in nature, clear asymmetries of ENSO events are seen between their cold and warm phases, including intensity, spatial patterns and period. This discrepancy can be partly attributed to the fact that the atmospheric statistical representations for interannual wind anomalies in our model preclude the effects of stochastic wind forcing (Zhang et al., 2008). In terms of SST variability, our HCM AOPB indeed has systematic biases in simulating the spatial patterns of ENSO compared with observations. For instance, the large amplitude of simulated interannual SST anomalies takes place in the central equatorial Pacific, whereas that of observed strong SST variability during typical ENSO events occurs in the eastern equatorial Pacific. So, the biases seen in the simplified HCM AOPB simulations may modify conclusions qualitatively. These issues need to be analyzed in the future.

Here, we demonstrate that Chl can have two-fold counteracting effects on ENSO at interannual and TIW scales in the tropical Pacfic. The amplitudes of ENSO can be modulated to be reduced by the Chl_{inter} perturbations, but to be increased by Chl_{TIW} perturbations, respectively. Then, the net effects induced by the combined Chl_{inter} and Chl_{TIW} effects can be different from those induced individually. Nevertheless, these results rely on only one-model simulations. Indeed, different models indicate large uncertainties in the represented amplitudes of bio-feedback onto SST. Due to the highly model-dependence of the modulating effects on ENSO by Chl, it is necessary to make validations using different models; the approach presented in this modeling study can be used in other modeling experiments. As de-

monstrated in our previous studies (e.g., Kang et al., 2017), for example, the SST_{TIW}-Chl_{TIW} and SST_{inter}-Chl_{inter} relationships can be constructed using statistical methods from satellite data, and then their effects can be adequately represented to take into account the Chl_{TIW} and Chl_{inter} influences in climate models even though ocean biogeochemistry processes are not explicitly included. In addition, in this study, we put our focus on the amplitude modulations of ENSO; nevertheless, ENSO also exhibits other properties that can be modulated by the related feedbacks. For example, observed SST interannual variability exhibits strong asymmetries during ENSO cycles, including amplitude and evolution between El Niño and La Niña events. These issues need to be carefully addressed due to the modulating effects on ENSO associated with TIW-induced Chl feedback. In addition, interactions of Chl effects with other processes, such as freshwater flux forcing (Kang et al., 2017), also need to be collectively taken into account when considering modulating effects on ENSO.

Acknowledgements *The authors wish to thank the two anonymous reviewers for their comments and suggestions that helped to improve the original manuscript. All figures in the main text are created by the authors using the Grid Analysis and Display System (GrADS) which is available at http://www.iges.org/grads/grads.html; the simulation data and scripts to create figures are available upon figshare (https://doi.org/10.6084/m9.figshare.11559369). Zhang Rong-Hua is supported by the National Natural Science Foundation of China (Grant No. 42030410), the Laoshan Laboratory Program (Grant No. LSKJ202202402), the Strategic Priority Research Program of the Chinese Academy of Sciences (Grant No. XDB40000000), the Startup Foundation for Introducing Talent of NUIST, and the Research Fund for Numerical Forecast Models of China Meteorological Administration (Grant No. CXFZ2022M001). Tian Feng is supported by the National Natural Science Foundation of China (Grant No. 42006001) and the Strategic Priority Research Program of the CAS (Grant Nos. XDB42040100 & XDB42040103).*

References

Adler R F, Huffman G J, Chang A, Ferraro R, Xie P P, Janowiak J, Rudolf B, Schneider U, Curtis S, Bolvin D, Gruber A, Susskind J, Arkin P, Nelkin E. 2003. The version-2 global precipitation climatology project (GPCP) monthly precipitation analysis (1979-present). J Hydrometeor, 4: 1147–1167

Baturin N G, Niiler P P. 1997. Effects of instability waves in the mixed layer of the equatorial Pacific. J Geophys Res, 102: 27771–27793

Bryden H L, Brady E C. 1989. Eddy momentum and heat fluxes and their effects on the circulation of the equatorial Pacific Ocean. J Mar Res, 47: 55–79

Chavez F P, Strutton P G, Friederich G E, Feely R A, Feldman G C, Foley D G, McPhaden M J. 1999. Biological and chemical response of the equatorial Pacific Ocean to the 1997–98 El Nino. Science, 286: 2126–2131

Chelton D B, Esbensen S K, Schlax M G, Thum N, Freilich M H, Wentz F J, Gentemann C L, McPhaden M J, Schopf P S. 2001. Observations of coupling between surface wind stress and sea surface temperature in the Eastern Tropical Pacific. J Clim, 14: 1479–1498

Chen D, Lian T, Fu C, Cane M A, Tang Y, Murtugudde R, Song X, Wu Q, Zhou L. 2015. Strong influence of westerly wind bursts on El Niño diversity. Nat Geosci, 8: 339–345

Collins M, An S I, Cai W, Ganachaud A, Guilyardi E, Jin F F, Jochum M, Lengaigne M, Power S, Timmermann A, Vecchi G, Wittenberg A. 2010. The impact of global warming on the tropical Pacific Ocean and El Niño. Nat Geosci, 3: 391–397

Gao C, Zhang R H, Karnauskas K B, Zhang L, Tian F. 2020. Separating freshwater flux effects on ENSO in a hybrid coupled model of the tropical Pacific. Clim Dyn, 54: 4605–4626

Gent P R, Cane M A. 1989. A reduced gravity, primitive equation model of the upper equatorial ocean. J Comput Phys, 81: 444–480

Gnanadesikan A, Anderson W G. 2009. Ocean water clarity and the ocean general circulation in a coupled climate model. J Phys Oceanog, 39: 314–332

Gorgues T, Menkes C, Aumont O, Vialard J, Dandonneau Y, Bopp L. 2005. Biogeochemical impact of tropical instability waves in the equatorial Pacific. Geophys Res Lett, 32: L24615

Hashizume H, Xie S, Liu W T, Takeuchi K. 2001. Local and remote atmospheric response to tropical instability waves: A global view from space. J Geophys Res, 106: 10173–10185

Holmes R M, McGregor S, Santoso A, England M H. 2019. Contribution of tropical instability waves to ENSO irregularity. Clim Dyn, 52: 1837–1855

Hu Z Z, Kumar A, Huang B, Zhu J, Zhang R H, Jin F F. 2017. Asymmetric evolution of El Niño and La Niña: The recharge/discharge processes and role of the off-equatorial sea surface height anomaly. Clim Dyn, 49: 2737–2748

Jochum M, Yeager S, Lindsay K, Moore K, Murtugudde R. 2010. Quantification of the feedback between phytoplankton and ENSO in the community climate system model. J Clim, 23: 2916–2925

Kang X, Zhang R H, Gao C, Zhu J. 2017. An improved ENSO simulation by representing chlorophyll-induced climate feedback in the NCAR Community Earth System Model. Sci Rep, 7: 17123

Kessler W S, Rothstein L M, Chen D. 1998. The annual cycle of SST in the eastern tropical Pacific, diagnosed in an ocean GCM. J Clim, 11: 777–799

Legeckis R. 1977. Long waves in the Eastern Equatorial Pacific Ocean: A view from a geostationary satellite. Science, 197: 1179–1181

Legeckis R, Brown C W, Bonjean F, Johnson E S. 2004. The influence of tropical instability waves on phytoplankton blooms in the wake of the Marquesas Islands during 1998 and on the currents observed during the drift of the Kon-Tiki in 1947. Geophys Res Lett, 31: 1–4

Lengaigne M, Menkes C, Aumont O, Gorgues T, Bopp L, André J M, Madec G. 2007. Influence of the oceanic biology on the tropical Pacific climate in a coupled general circulation model. Clim Dyn, 28: 503–516

Lian T, Chen D K, Tang Y M. 2017. Genesis of the 2014–2016 El Niño events. Sci China Earth Sci, 60: 1589–1600

Maritorena S, Siegel D A. 2005. Consistent merging of satellite ocean color data sets using a bio-optical model. Remote Sens Environ, 94: 429–440

Marzeion B, Timmermann A, Murtugudde R, Jin F F. 2005. Biophysical feedbacks in the tropical Pacific. J Clim, 18: 58–70

Menkes C E. 2002. A whirling ecosystem in the equatorial Atlantic. Geophys Res Lett, 29: 1553

Miller A J, Alexander M A, Boer G J, Chai F, Denman K, Erickson Iii D J, Frouin R, Gabric A J, Laws E A, Lewis M R, Liu Z, Murtugudde R, Nakamoto S, Neilson D J, Norris J R, Ohlmann J C, Perry R I, Schneider N, Shell K M, Timmermann A. 2003. Potential feedbacks between Pacific Ocean ecosystems and interdecadal climate variations. Bull Amer Meteor Soc, 84: 617–634

Murtugudde R, Beauchamp J, McClain C R, Lewis M, Busalacchi A J. 2002. Effects of penetrative radiation on the upper tropical ocean circulation. J Clim, 15: 470–486

Park J Y, Kug J S, Park Y G. 2014. An exploratory modeling study on biophysical processes associated with ENSO. Prog Oceanography, 124: 28–41

Reynolds R W, Rayner N A, Smith T M, Stokes D C, Wang W. 2002. An improved in situ and satellite SST analysis for climate. J Clim, 15: 1609–1625

Shi Q, Zhang R H, Tian F. 2023. Impact of the deep chlorophyll maximum

in the equatorial Pacific as revealed in a coupled ocean gcm-ecosystem model. J Geophys Res-Oceans, 128: e2022JC018631
Strutton P G, Ryan J P, Chavez F P. 2001. Enhanced chlorophyll associated with tropical instability waves in the equatorial Pacific. Geophys Res Lett, 28: 2005–2008
Tian F, Zhang R H, Wang X. 2018. A coupled ocean physics-biology modeling study on tropical instability wave-induced chlorophyll impacts in the Pacific. J Geophys Res-Oceans, 123: 5160–5179
Tian F, Zhang R H, Wang X. 2019. A positive feedback onto ENSO due to Tropical Instability Wave (TIW)-Induced chlorophyll effects in the Pacific. Geophys Res Lett, 46: 889–897
Timmermann A, Jin F F. 2002. Phytoplankton influences on tropical climate. Geophys Res Lett, 29: 19-1–19-4
Wang X, Le Borgne R, Murtugudde R, Busalacchi A J, Behrenfeld M. 2009. Spatial and temporal variability of the phytoplankton carbon to chlorophyll ratio in the equatorial Pacific: A basin-scale modeling study. J Geophys Res, 114: C07008
Wang X, Murtugudde R, Hackert E, Wang J, Beauchamp J. 2015. Seasonal to decadal variations of sea surface p CO_2 and sea-air CO_2 flux in the equatorial oceans over 1984–2013: A basin-scale comparison of the Pacific and Atlantic Oceans. Glob Biogeochem Cycle, 29: 597–609
Wetzel P, Maier-Reimer E, Botzet M, Jungclaus J, Keenlyside N, Latif M. 2006. Effects of ocean biology on the penetrative radiation in a coupled climate model. J Clim, 19: 3973–3987
Xie S P. 2004. Satellite observations of cool ocean-atmosphere interaction. Bull Am Meteorol Soc, 85: 195–208
Yu J Y, Kim S T. 2010. Three evolution patterns of Central-Pacific El Niño. Geophys Res Lett, 37: L08706
Yu L, Weller R A. 2007. Objectively analyzed air-sea heat fluxes for the global ice-free oceans (1981–2005). Bull Am Meteorol Soc, 88: 527–540
Zhang R H. 2014. Effects of tropical instability wave (TIW)-induced surface wind feedback in the tropical Pacific Ocean. Clim Dyn, 42: 467–485
Zhang R H. 2015. An ocean-biology-induced negative feedback on ENSO as derived from a hybrid coupled model of the tropical Pacific. J Geophys Res-Oceans, 120: 8052–8076
Zhang R H, Busalacchi A J, DeWitt D G. 2008. The roles of atmospheric stochastic forcing (SF) and oceanic entrainment temperature (Te) in decadal modulation of ENSO. J Clim, 21: 674–704
Zhang R H, Busalacchi A J, Wang X, Ballabrera-Poy J, Murtugudde R G, Hackert E C, Chen D. 2009. Role of ocean biology-induced climate feedback in the modulation of El Niño-Southern Oscillation. Geophys Res Lett, 36: L03608
Zhang R H, Gao C. 2016. The IOCAS intermediate coupled model (IOCAS ICM) and its real-time predictions of the 2015–2016 El Niño event. Sci Bull, 61: 1061–1070
Zhang R H, Rothstein L M, Busalacchi A J. 1998. Origin of upper-ocean warming and El Niño change on decadal scales in the tropical Pacific Ocean. Nature, 391: 879–883
Zhang R H, Tian F, Busalacchi A J, Wang X. 2019a. Freshwater flux and ocean chlorophyll produce nonlinear feedbacks in the tropical Pacific. J Clim, 32: 2037–2055
Zhang R H, Tian F, Wang X. 2018. A new hybrid coupled model of atmosphere, ocean physics, and ocean biogeochemistry to represent biogeophysical feedback effects in the tropical Pacific. J Adv Model Earth Syst, 10: 1901–1923
Zhang R H, Tian F, Zhi H, Kang X. 2019b. Observed structural relationships between ocean chlorophyll variability and its heating effects on the ENSO. Clim Dyn, 53: 5165–5186
Zhang R H, Yu Y, Song Z, Ren H L, Tang Y, Qiao F, Wu T, Gao C, Hu J, Tian F, Zhu Y, Chen L, Liu H, Lin P, Wu F, Wang L. 2020. A review of progress in coupled ocean-atmosphere model developments for ENSO studies in China. J Ocean Limnol, 38: 930–961
Zhang R H, Zheng F, Zhu J, Pei Y, Zheng Q, Wang Z. 2012. Modulation of El Niño-Southern Oscillation by freshwater flux and salinity variability in the tropical Pacific. Adv Atmos Sci, 29: 647–660
Zhang R H, Busalacchi A J. 2009a. An empirical model for surface wind stress response to SST forcing induced by tropical instability waves (TIWs) in the eastern equatorial Pacific. Mon Weather Rev, 137: 2021–2046
Zhang R H, Busalacchi A J. 2009b. Freshwater flux (FWF)-induced oceanic feedback in a hybrid coupled model of the tropical Pacific. J Clim, 22: 853–879
Zhu J, Huang B, Marx L, Kinter Iii J L, Balmaseda M A, Zhang R H, Hu Z Z. 2012. Ensemble ENSO hindcasts initialized from multiple ocean analyses. Geophys Res Lett, 39: L09602
Zhu J, Huang B, Zhang R H, Hu Z Z, Kumar A, Balmaseda M A, Marx L, Kinter III J L. 2014. Salinity anomaly as a trigger for ENSO events. Sci Rep, 4: 6821

(Editorial handling: Dake CHEN)